



GASTROINTESTINAL, HEPATOBILIARY, AND PANCREATIC PATHOLOGY

***Bifidobacteria* Stabilize Claudins at Tight Junctions and Prevent Intestinal Barrier Dysfunction in Mouse Necrotizing Enterocolitis**

Kelly R. Bergmann,^{*} Shirley X.L. Liu,^{*} Runlan Tian,^{*} Anna Kushnir,^{*} Jerrold R. Turner,[†] Hong-Lin Li,[‡] Pauline M. Chou,[§] Christopher R. Weber,[†] and Isabelle G. De Plaen^{*}

From the Division of Neonatology,^{*} Department of Pediatrics, and the Department of Pathology,[§] Ann & Robert H. Lurie Children's Hospital of Chicago Research Center, Northwestern University Feinberg School of Medicine, Chicago, Illinois; the Department of Pathology,[†] University of Chicago Pritzker Medical School of Medicine, Chicago, Illinois; and the Department of Biochemistry and Molecular Biology,[‡] Cancer Center, Georgia Health Sciences University, Augusta, Georgia

Accepted for publication
January 7, 2013.

Address correspondence to
Isabelle G. De Plaen, M.D.,
Department of Pediatrics,
Division of Neonatology, Ann
& Robert H. Lurie Children's
Hospital of Chicago, 225 E.
Chicago Ave., #45, Chicago, IL
60611. E-mail: isabelledp@northwestern.edu.

Whether intestinal barrier disruption precedes or is the consequence of intestinal injury in necrotizing enterocolitis (NEC) remains unknown. Using a neonatal mouse NEC model, we examined the changes in intestinal permeability and specific tight-junction (TJ) proteins preceding NEC and asked whether these changes are prevented by administration of *Bifidobacterium infantis*, a probiotic known to decrease NEC incidence in humans. Compared with dam-fed controls, pups submitted to the NEC protocol developed i) significantly increased intestinal permeability at 12 and 24 hours (as assessed by 70-kDa fluorescein isothiocyanate—dextran transmucosal flux); ii) occludin and claudin 4 internalization at 12 hours (as assessed by immunofluorescence and low-density membrane fraction immunoblotting); iii) increased claudin 2 expression at 6 hours and decreased claudin 4 and 7 expression at 24 hours; and iv) increased claudin 2 protein at 48 hours. Similar results were seen in human NEC, with claudin 2 protein increased. In mice, administration of *B. infantis* micro-organisms attenuated increases in intestinal permeability, preserved claudin 4 and occludin localization at TJs, and decreased NEC incidence. Thus, an increase in intestinal permeability precedes NEC and is associated with internalization of claudin 4 and occludin. Administration of *B. infantis* prevents these changes and reduces NEC incidence. The beneficial effect of *B. infantis* is, at least in part, due to its TJ and barrier-preserving properties. (*Am J Pathol* 2013, 182: 1595–1606; <http://dx.doi.org/10.1016/j.ajpath.2013.01.013>)

Necrotizing enterocolitis (NEC) is one of the most common gastrointestinal diseases among premature infants, affecting approximately 7% of infants weighing <1500 g.¹ The precise etiology of NEC is unknown, although it is thought to be a multifactorial disease with prematurity, enteral feeding, hypoxic—ischemic injury, and abnormal bacterial colonization as contributing risk factors.¹ Although studies in both rats and humans have shown that NEC results in significant gut barrier dysfunction late in its course,^{2–4} the question remained whether increased intestinal permeability precedes or is the consequence of bowel injury.

Intestinal permeability is regulated by intercellular structures termed tight junctions (TJs). These form a selectively permeable intercellular barrier at the apical aspect of the

enterocyte lateral membranes and regulate the paracellular movement of molecules between the intestinal lumen and subepithelial tissues.⁵ TJs are composed of numerous structural and functional proteins, of which the claudin family is known to control charge selectivity and ion and small molecule permeability.^{6,7} Mutations in claudins have been shown to disrupt paracellular transport.⁸ Alterations in TJ proteins may lead to mucosal barrier disruption and contribute to the mechanism by which pathogens and foreign antigens cross

Supported by NIH grants K08-HD044558, R01-HD060876-01A1 (I.G.D.P.), R01-DK061931, R01-DK068271 (J.R.T.), an Illinois Department of Public Aid grant (I.G.D.P.), the American Gastroenterological Association bridge fund (I.G.D.P.), and a Society for Pediatric Research summer student award (K.R.B.).

the epithelial barrier.⁹ Studies in both animals and humans have shown that inflammatory bowel disease is associated with changes in claudin expression and localization.^{10,11} Similarly, altered expression of the TJ protein claudin 3 has been found at day 3 in a neonatal rat model of NEC.^{3,12,13} At that time point, however, pups exhibit obvious injury in the distal ileum, with dilation, severe hemorrhage, and gross discoloration.³ TJ protein expression and distribution before gross intestinal injury have not previously been characterized in NEC.

The newborn intestine is sterile at birth, but within 24 hours it becomes colonized with microbes derived from the maternal birth canal and the external environment.¹⁴ In breastfed neonates, gut colonization with various species of *Bifidobacterium* occurs between 4 days and 2 weeks of life.¹⁴ The proportion of *Bifidobacterium* species is reduced in the intestine of formula-fed infants.¹⁵ Prematurity is associated with a delay in the establishment of bifidobacterial flora,¹⁶ which may predispose the premature intestine to NEC. Rat and human studies have shown that prophylactic administration of *B. infantis* and other probiotics reduces the incidence and severity of NEC.^{17,18} The mechanisms of action of probiotics are multifaceted and may include the following: preventing bacterial overgrowth, providing a physical barrier to pathogenic bacterial colonization, modifying intestinal pH, modulating the immune system through increased IgA or cytokine regulation, and intestinal barrier regulation.¹⁹ The mechanism by which *B. infantis* protects the neonatal intestine against NEC has been poorly understood.

In the present study, we used a neonatal mouse NEC model induced by bacterial inoculation, hypoxia-cold stress, and formula feeding to determine i) whether intestinal permeability is increased within 24 hours, before the occurrence of intestinal injury, ii) whether the increase in permeability is associated with changes in TJ protein expression and localization, iii) whether any such TJ protein changes correlate with human NEC, and iv) whether *B. infantis* prevents intestinal injury, alteration of TJ, and epithelial barrier dysfunction.

Materials and Methods

Animal Model

NEC was induced using a neonatal mouse model previously characterized by our research group.²⁰ Briefly, naturally delivered C57BL/6 newborn mice (pups) were placed in a humidified neonatal incubator at 37°C and were inoculated with 10⁷ colony-forming units (CFU) of a standardized adult commensal bacteria mixture within 12 hours of birth.²⁰ Pups were then gavaged with 30 µL Esbilac (PetAg, Inc., Hampshire, IL) formula (33 g diluted in 100 mL of water) every 3 hours and submitted to brief episodes of asphyxia (100% N₂ for 60 seconds) and cold stress (10 minutes at 4°C) twice per day. With this protocol, 70% to 80% of pups develop clinical

signs similar to NEC within 72 hours.²⁰ For probiotic studies, pups were treated with *B. infantis* strain BB-02 (3 × 10⁶ CFU in 20 µL), diluted in either dextrose (for initial immunofluorescence studies) or maltodextran (for later permeability, Western blot, and histology studies) before being submitted to the NEC protocol. The *B. infantis* microorganisms, freeze-dried from a human source, were provided by Chr. Hansen A/S (Hoersholm, Denmark).

To test the effect of *B. infantis* on NEC incidence, litters were divided into two groups of matched weight and genetic background. One group was treated with *B. infantis* and the other with vehicle alone; both groups were submitted to the NEC protocol. Pups were closely observed and euthanized by decapitation at 72 hours or when showing signs of distress such as severe abdominal distension, respiratory distress, or lethargy. The small intestines were collected and fixed in buffered formalin for histological examination. Microscopic injury was graded in a masked fashion, as described previously.²⁰ Animal experiments were approved by the Ann & Robert H. Lurie Children's Hospital of Chicago Research Center Institutional Animal Care and Use Committee.

Human Small Intestinal and Colonic Tissue Staining

Patient samples were obtained under protocols approved by the University of Chicago Institutional Review Board and Ann & Robert H. Lurie Children's Hospital of Chicago (formerly named: Children's Memorial Hospital) Institutional Review Board. Formalin-fixed, paraffin-embedded tissues obtained from segmental resections of 40 infants under 10 weeks of age were colon controls (*n* = 11), colon NEC cases (*n* = 10), small intestine controls (*n* = 9), and small intestine NEC cases (*n* = 10). Control samples were tissues resected during surgical intervention for ileal atresia, intestinal reanastomosis, duplication cyst, or Hirschsprung's disease. Immunohistochemical stains for claudins 2 and 4, occludin, and zona occludens-1 (ZO-1) were performed on formalin-fixed, paraffin-embedded tissue sections (4 µm thick), as described previously.²¹ Staining intensity of all immunostains was scored semiquantitatively from 0 to 3 by two separate observers (I.G.D.P. and C.R.W.) and average scores were used. In the rare instance when scores between the two observers were discordant by more than one point, the sample was rescored at a two-headed microscope and a consensus was achieved.

Intestinal Permeability

Pups were fasted for 2 hours and gavaged with 750 mg/kg of fluorescein isothiocyanate (FITC)—conjugated dextran (70 kDa; Sigma-Aldrich, St. Louis, MO).¹⁷ Animals were sacrificed 4 hours later, and whole blood (50 µL) and small intestines were collected. Serum fluorescence was measured, and values were compared with serial dilutions of known FITC—dextran concentrations.

Electron Microscopy

Murine small intestinal tissues were fixed in 3% glutaraldehyde, postfixed in 2% osmium tetroxide, and embedded in epoxy resin. Sections were stained with lead citrate and uranyl acetate and were studied under a Zeiss M-10 electron microscope (Carl Zeiss Microscopy, Jena, Germany). TJ lengths were measured in images oriented parallel to the axis of microvilli by a pathologist masked to group assignment (C.R.W.).

qPCR

Total cellular RNA was extracted from murine intestinal tissue. cDNA was synthesized and purified as described previously.²² Quantitative real-time PCR (qPCR) was performed using a QuantiTect SYBR Green PCR kit (Qiagen, Valencia, CA),²² with the following primer sequences: claudin 1 forward: 5'-TCTACGAGGGACTGTGGATG-3'; claudin 1 reverse: 5'-TCAGATTCAGCAAGGAGTCCG-3'; claudin 2 forward: 5'-GGCTGTTAGGCACATCCAT-3'; claudin 2 reverse: 5'-TGGCACCAACATAGGAAGTCT-3'; claudin 3 forward: 5'-AAGCCGAATGGACAAAGAA-3'; claudin 3 reverse: 5'-CTGGCAAGTAGCTGCAGTG-3'; claudin 4 forward: 5'-CGCTACTCTTGCCATTACG-3'; claudin 4 reverse: 5'-ACTCAGCACACCATGACTTG-3'; claudin 5 forward: 5'-GTGGAACGCTCAGATTTCAT-3'; claudin 5 reverse: 5'-TGGACATTAAGGCAGCATCT-3'; claudin 7 forward: 5'-AGGGTCTGCTCTGGTCCTT-3'; claudin 7 reverse: 5'-GTACGCAGCTTTGCTTTCA-3'; claudin 8 forward: 5'-GCCGGAATCATCTTCTTCAT-3'; claudin 8 reverse: 5'-CATCCACCAGTGGGTTGTAG-3'; claudin 10 forward: 5'-CCCAGAATGGGCTACACATA-3'; claudin 10 reverse: 5'-CCTTCTCCGCCTTGATACTT-3'; claudin 12 forward: 5'-GTCCTCTCCTTTCTGGCAAC-3'; claudin 12 reverse: 5'-ATGTCGATTTCAATGGCAGA-3'; claudin 14 forward: 5'-GCTCCTAGGCTTCTGCTTA-3'; claudin 14 reverse: 5'-CTGGTAGATGCCTGTGCTGT-3'; claudin 15 forward: 5'-CAGCTTCGGTAAATATGCCA-3'; claudin 15 reverse: 5'-CAGTGGGACAAGAAATGGTG-3'; occludin forward: 5'-GCTGTGATGTGTGTGAGCTG-3'; occludin reverse: 5'-GACGGTCTACCTGGAGGAAC-3'; ZO-1 forward: 5'-AGGACACCAAAGCATGTGAG-3'; ZO-1 reverse: 5'-GGCATTCCTGCTGGTTACA-3'; K8 reverse: 5'-AAGGTTGGCCAGAGGATTAGG-3'; K8 forward: 5'-CTCCTGCAGCTGTATGGCAG-3'. For each group, three to eight samples were run in duplicate. Gene expression was normalized to the housekeeping gene keratin 8 (K8), which was consistent between runs.

Western Blotting

For Western blotting, 10 µg of total protein was used for Western blotting, as described previously.²² Scanned gels were analyzed using Adobe (San Jose, CA) Photoshop CS4 extended edition software, and the protein/β-actin ratio was determined from the background-corrected integrated band densities.

Immunofluorescence

Immunostaining was performed as described previously.²³ Frozen sections (5 µm thick) were placed on coated slides, fixed in 1% paraformaldehyde, and washed three times in 1× PBS. Nonspecific binding was blocked with 10% normal goat serum containing 50 µg/mL purified rat anti-mouse CD16/CD32 (Mouse BD Fc block; BD Pharmingen, San Jose, CA; catalog no. 553142). Sections were incubated with 2.5 µg/mL mouse anti-claudin 2 (catalog no. 32-5600), 1.25 µg/mL rabbit anti-claudin 4 (catalog no. 36-4800), 1.25 µg/mL rabbit anti-claudin 7 (catalog no. 34-9100), or 1.25 µg/mL rabbit anti-occludin (C-terminal)

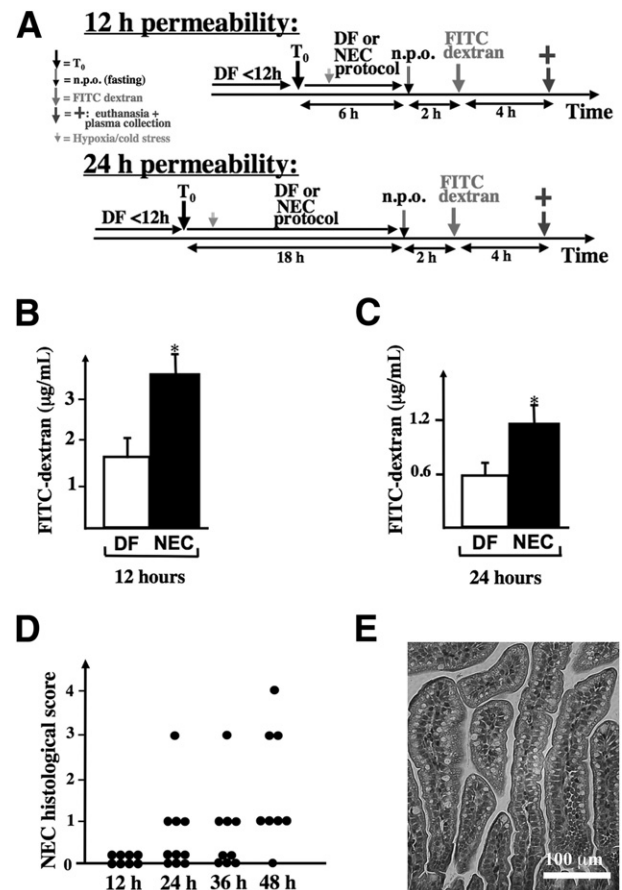


Figure 1 Intestinal permeability is increased in NEC at 12 and 24 hours, before histological changes of NEC are detected. **A:** Pups were randomized into two groups at time T₀: group 1 (DF) was left with the dams as controls, and group 2 (NEC) was stressed according to the NEC protocol. Six hours before euthanasia, pups were fasted for 2 hours, and then 750 mg/kg (diluted in 25 µL of 0.9% NaCl) FITC-dextran (70 kDa) was administered through an orogastric tube. **B** and **C:** At the time of euthanasia, 50 µL of whole blood was collected, and serum FITC-dextran concentration was determined at 12 hours (**B**) and 24 hours (**C**). **D:** Histological grade of the small intestine of mice submitted to the NEC protocol and euthanized at different time points (every 12 hours). **E:** Typical appearance of the intestine after 24 hours on the NEC protocol, showing absence of villous injury. Data in **B** and **C** are expressed as means ± SEM. *n* = 7 to 11 per group. **P* < 0.05. Scale bar = 100 µm.

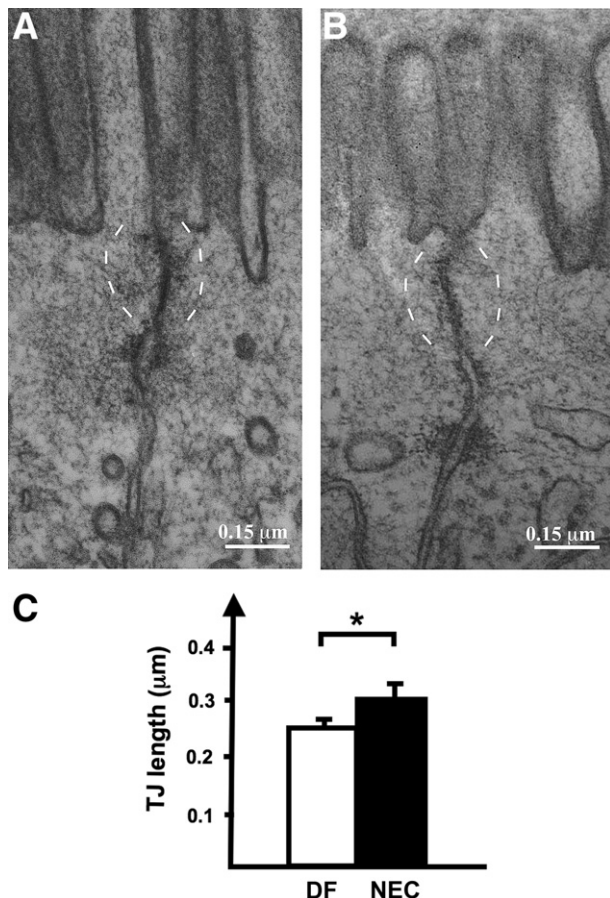


Figure 2 Small intestine epithelial cell TJ regions in controls and stressed pups. **A** and **B**: At 24 hours, electron micrographs reveal intact TJs (delineated by **dashed brackets**) in both DF controls (**A**) and pups stressed on the NEC protocol (**B**). The apical-to-basolateral TJ length was longer in pups stressed for 24 hours (**B**) than in DF controls (**A**). **C**: Mean TJ length was measured by a pathologist (C.R.W.) masked to group assignment. Data are expressed as means \pm SEM. $n = 16$ (DF control) or 13 (stressed pups). * $P < 0.05$. Scale bar = 0.15 μm .

(catalog no. 42-2400) antibodies for 3 hours, washed and incubated with Alexa Fluor 488–conjugated phalloidin at 1:1000 (catalog no. A12379), Alexa Fluor 594 goat anti-rabbit IgG at 1:750 (catalog no. A11037), and DAPI (catalog no. P36931), all from Life Technologies–Invitrogen (Grand Island, NY). Sections were imaged using a DMLB epifluorescence microscope (Leica Microsystems, Wetzlar, Germany) equipped with a Retiga EXI camera (QImaging, Surrey, BC, Canada) controlled by MetaMorph software version 7 (Universal Imaging, Marlow, UK).

Subcellular Fractionation

Subcellular fractionation was performed as described previously.²³ Briefly, intestinal tissues were lysed in Tris-buffered saline containing 1% Triton X-100. Lysate (3.2 mL in 40% sucrose) was layered over an 0.8-mL cushion of 50% sucrose. Decreasing sucrose concentration layers were

added over the lysate, as follows: 1.6 mL of 35% sucrose, 1.6 mL of 30% sucrose, 2.4 mL of 15% sucrose, and 0.8 mL of 5% sucrose. Gradients were centrifuged at $280,000 \times g$ for 18 hours at 4°C. Collected fractions were analyzed using Western blotting. Sucrose concentration was measured by densitometry, and total protein of the fractions was measured with a Bio-Rad protein assay (Bio-Rad Laboratories, Hercules, CA).

Statistical Analysis

Student's *t*-test was used to compare mean permeability between murine groups and to compare differences in expression between human tissue groups. A two-sided Wilcoxon–Mann–Whitney test was used to compare ΔC_T values (for qPCR) and background-corrected integrated density

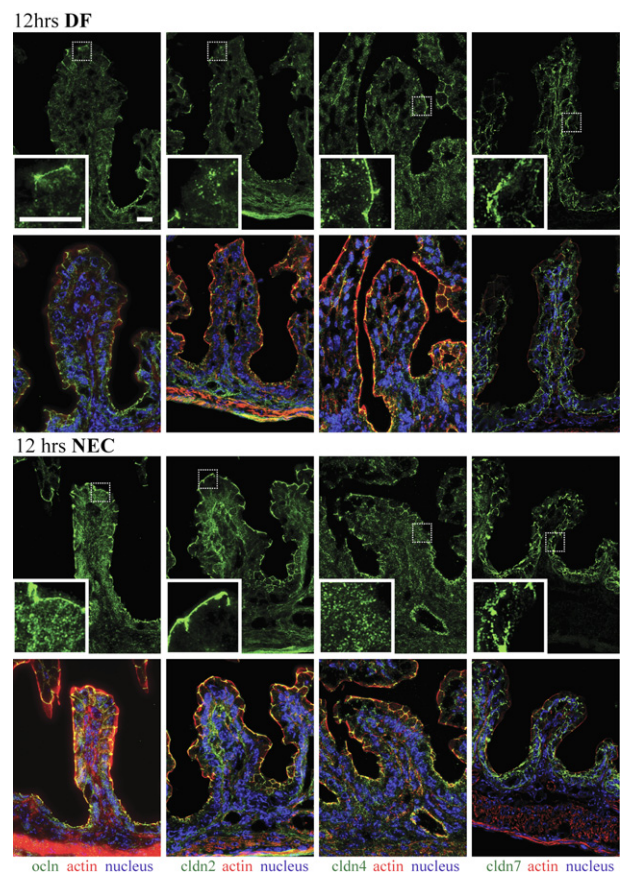


Figure 3 Internalization of claudin 4 and occludin in enterocytes of stressed pups at 12 hours. Frozen sections of small intestines of pups submitted to the NEC protocol or DF controls were examined for occludin (ocln, green) and claudins (cldn, green) 2, 4, and 7 by immunofluorescence (**top row** in each group). **Boxed regions** correspond to higher-magnification images in the **insets**. Merged images (**bottom row** in each group) also show β -actin (red) and DAPI nuclear staining (blue). In DF mice, claudin 2, claudin 4, and occludin were present mainly at TJs, and claudin 7 was detected along cellular membranes. In pups stressed for 12 hours, occludin and claudin 4 were found throughout the cytoplasm. Claudin 2 was largely associated with TJs while claudin 7 was found along the cellular membranes as in dam fed controls. $n = 3$ to 6 per group. Scale bar = 40 μm .

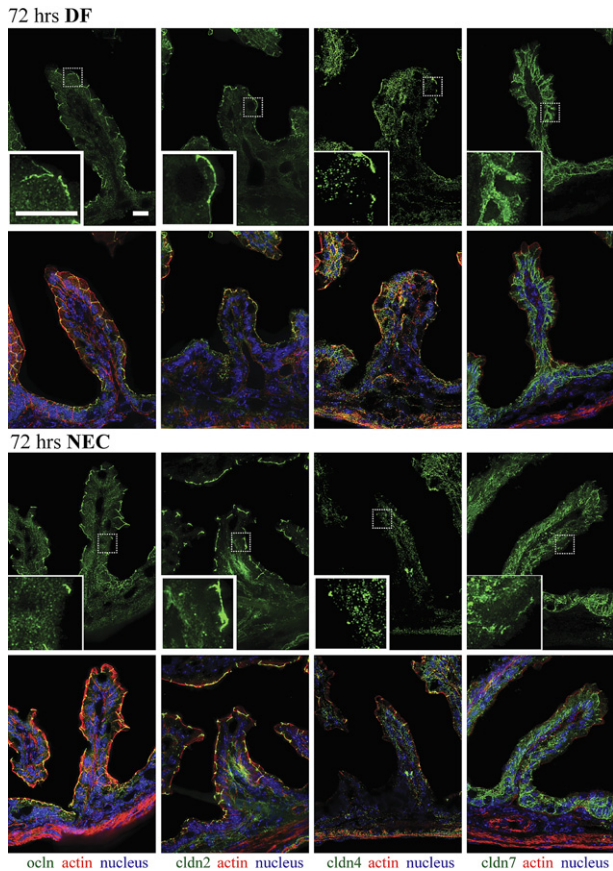


Figure 4 Internalization of claudins 2, 4, and 7 and occludin in enterocytes of stressed pups at 72 hours. Frozen sections of small intestines of pups submitted to the NEC protocol or DF controls were examined for occludin (green) and claudins (green) 2, 4, and 7 by immunofluorescence (**top row** in each group). Merged images (**bottom row** in each group) also show β -actin (red) and DAPI nuclear staining (blue). In DF mice, claudin 2, 4, and occludin were present mainly at TJs, and claudin 7 was detected along cellular membranes. In pups stressed for 72 hours, occludin and claudins 2, 4, and 7 were found throughout the cytoplasm; the association of claudins 2 and 4 with TJs was decreased, whereas the association of occludin with TJs was only focally decreased in villi and a small amount was found throughout the cytoplasm. $n = 3$ to 6 per group. Scale bar = 40 μ m.

values (for Western blot densitometry). The χ^2 analysis was used to evaluate the differences in NEC incidence between the two groups. Data are expressed as means \pm SEM. $P < 0.05$ was considered significant.

Results

Intestinal Permeability Is Increased at 12 and 24 Hours, before the Onset of Histological Intestinal Injury, in a Neonatal Mouse NEC Model

To determine whether intestinal permeability is increased at 12 and 24 hours, serum FITC–dextran concentration was measured 4 hours after gastric administration of 750 mg/kg of FITC–dextran (70 kDa) in stressed pups or dam-fed (DF) controls (**Figure 1A**). Intestinal permeability (as reflected by a higher FITC–dextran serum concentration) was 2.12 ± 0.37 -fold greater at 12 hours ($P < 0.05$) (**Figure 1B**) and

1.95 ± 0.29 -fold greater at 24 hours ($P < 0.05$) (**Figure 1C**) in stressed animals, compared with DF controls. To confirm that intestinal injury was not present at these time points, we examined the intestine of pups submitted to the NEC model for

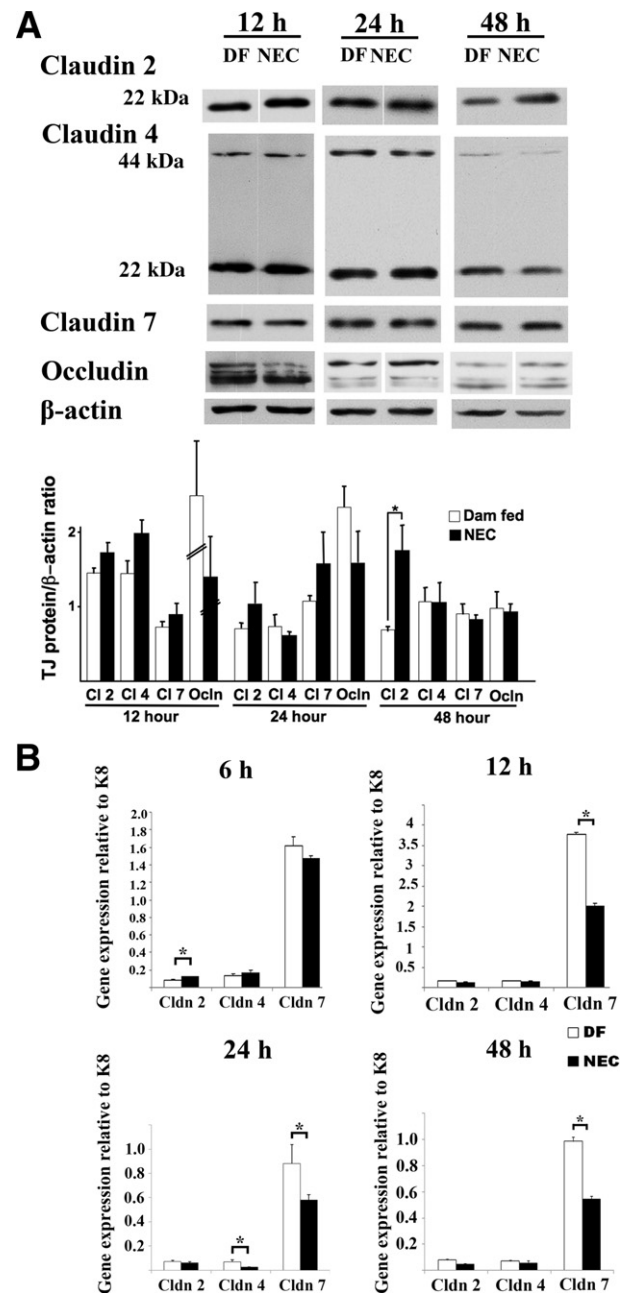


Figure 5 Claudin 2 protein levels are increased in the small intestine of stressed pups at 48 hours, claudin 2 gene expression is up-regulated at 6 hours, and claudin 4 and 7 gene expression is down-regulated at 24 hours, compared with DF controls. **A:** Presence of occludin and claudins 2, 4, and 7 in the small intestine of NEC stressed mouse pups versus DF controls at 12, 24, and 48 hours was analyzed by Western blotting. Membranes were then stripped and immunoblotted for β -actin, and the results were quantified. Similar results were obtained in two independent experiments. Nonadjacent lanes from the same blot are separated by a fine space. **B:** The gene expression profile of claudins 2, 4, and 7 relative to K8 was obtained by qPCR in DF versus stressed pups at 6, 12, 24, and 48 hours. Data are expressed as means \pm SEM. $n = 4$ samples per group (**A**) or 3 to 8 samples per group, run in duplicate (**B**). $*P < 0.05$. Cl, claudin.

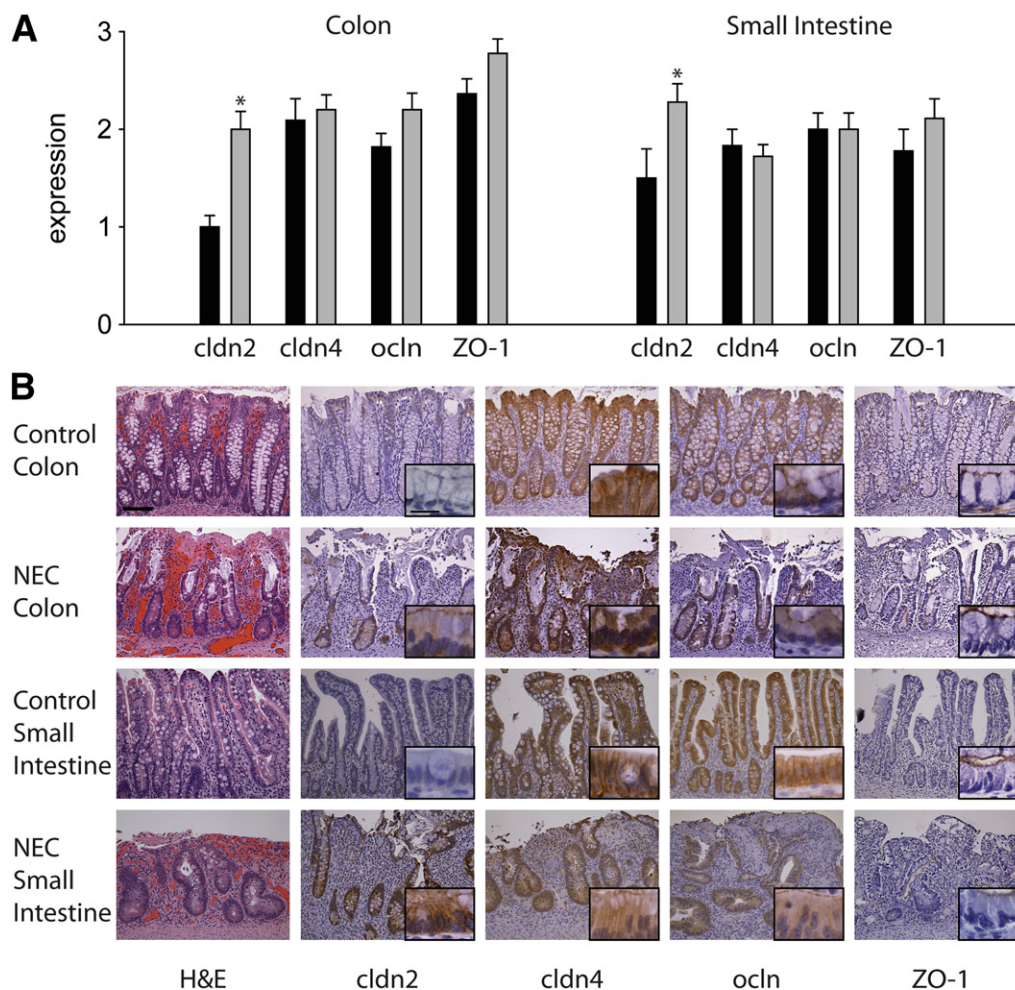


Figure 6 Claudin 2 expression is elevated in human NEC. **A:** Immunohistochemical staining in human control and NEC tissues was scored semiquantitatively from 0 to 3. **B:** In the crypts, the expression of claudin 2 was low in control colon and small intestine, but was increased in NEC tissues. In contrast, the expression of claudin 4, occludin, and ZO-1 was similar between control and NEC tissues. * $P \leq 0.05$; $n = 9$ to 11 per group. Scale bars: 100 μm (main images); 20 μm (insets).

12, 24, 36, or 48 hours by histology. None of the pups stressed for 12 hours had evidence of NEC. Only 1/10 pups had severe NEC (injury score ≥ 2) at 24 hours, 1/9 at 36 hours, and 3/8 at 48 hours (Figure 1D). Intestinal permeability was increased at 12 hours (Figure 1B), a time point at which no intestinal injury was observed (Figure 1, D and E); the permeability increase therefore precedes the intestinal injury in our model.

Stressed Pups Exhibit Intact TJ Structures with TJ Restructuring

Increased intestinal permeability in the absence of histological evidence of epithelial damage suggests a TJ defect. We therefore examined enterocyte TJ ultrastructure. At 24 hours, both stressed pups and DF controls exhibited adjacent membrane kisses, which are typical of intact TJ structures (Figure 2, A and B). The apical-to-basolateral TJ length was $23.6 \pm 1.6\%$ greater in tissues of stressed pups ($0.31 \pm 0.02 \mu\text{m}$) at 24 hours, compared with DF control tissues ($0.25 \pm 0.01 \mu\text{m}$) ($P < 0.05$), consistent with TJ restructuring (Figure 2C).

Claudins 2, 4, and 7 and Occludin Are Internalized in the Enterocytes of Neonatal Mice Submitted to the NEC Protocol

Among the many TJ proteins examined in our preliminary studies (data not shown), claudins 2, 4, and 7 were highly expressed in neonatal mouse intestinal tissues. We therefore chose to further examine these TJ proteins by immunofluorescence. In DF pups, claudin 2, claudin 4, and occludin were concentrated at TJ structures of enterocytes, with only a minimal amount detectable in the cytoplasm; claudin 7 was detected along lateral membranes (Figures 3 and 4). In pups stressed for 12 hours (Figure 3), occludin and claudin 4 were detected throughout the cytoplasm, and claudin 4 was significantly decreased at the TJ (Figure 3). In pups stressed for 24 hours (data not shown) and 72 hours (Figure 4), occludin, claudins 2, 4, and 7 were noted throughout the cytoplasm, with higher concentrations in the perinuclear and basal regions. In pups stressed for 24 hours (data not shown) and for 72 hours (Figure 4), the decreased association of

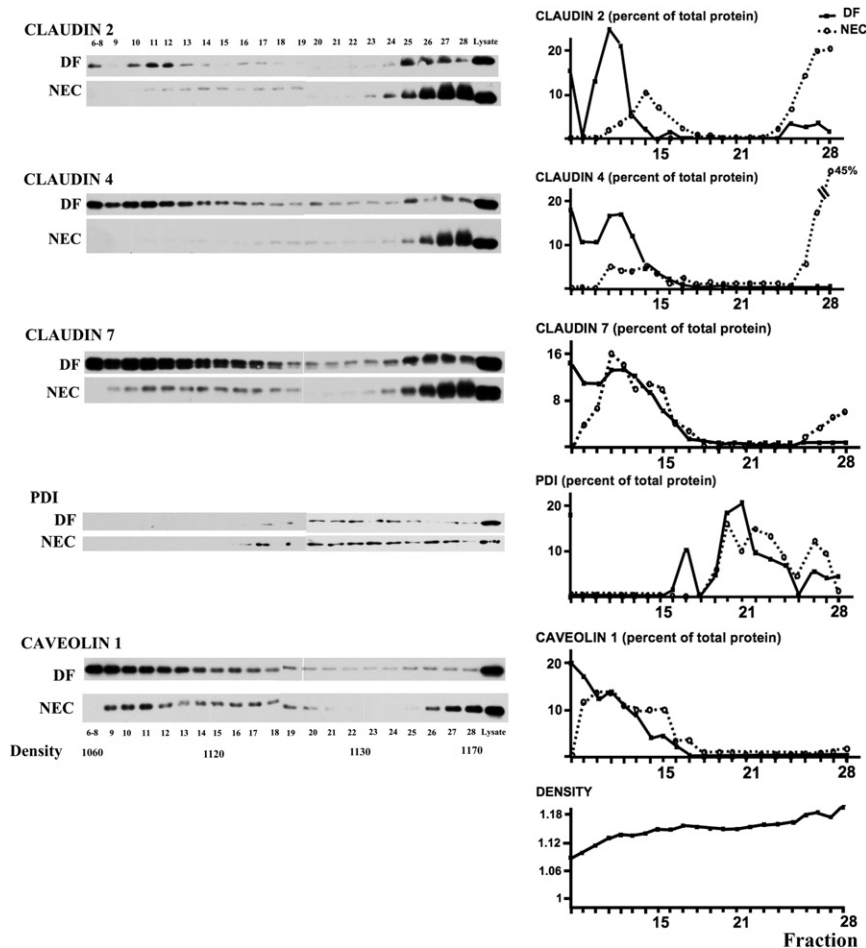


Figure 7 Redistribution of TJ proteins from membrane to high-density fractions in the small intestine of pups submitted to the NEC protocol for 24 hours. Subcellular fractions from small intestines of DF controls and stressed pups were separated by centrifugation on a discontinuous sugar density gradient and submitted to Western blotting and quantification of claudin proteins and specific subcellular markers. Protein disulfide isomerase (PDI) was used as an endoplasmic reticulum marker and caveolin 1 as a lipid raft marker. Results are representative of two independent experiments, run in triplicate.

claudin 4 with TJs remained, and the occludin association with TJs was focally decreased in villous enterocytes.

Claudin 2 Is Increased at 48 Hours in the Small Intestine of Stressed Pups, Compared with Dam-Fed Controls

Western blot analysis revealed a trend toward an increase in claudin 2 at 12 hours (claudin 2/ β -actin ratio = 1.78 ± 0.15 versus 1.44 ± 0.17 ; $P = 0.1$) and 24 hours (1.04 ± 0.24 versus 0.70 ± 0.06 ; $P = 0.60$) in stressed pups, compared with controls (Figure 5A). This increase in claudin 2 was significant at 48 hours (claudin 2/ β -actin ratio = 1.99 ± 0.38 in stressed pups versus 0.78 ± 0.05 in controls; $P < 0.05$) (Figure 5A). We did not observe any significant changes in the level of claudin 4, claudin 7, or occludin (Figure 5A).

Claudin 2 Gene Expression Is Up-Regulated at 6 Hours and Claudin 4, and Claudin 7 Gene Expression Is Down-Regulated in the Intestine of Stressed Pups at 24 Hours, Compared with Dam-Fed Controls

Claudin 2 expression, measured by qPCR and normalized to the epithelial cell marker K8, was significantly up-regulated,

by 50% (95% confidence interval, CI = 46 to 54%; $P < 0.05$), at 6 hours; claudin 7 expression was significantly down-regulated, by 42% (CI = 33% to 51%; $P < 0.05$), at 12 hours; and claudin 4 and claudin 7 expression was significantly down-regulated, by 63% (CI = 41% to 75%; $P < 0.05$) and 34% (CI = 12% to 56%; $P < 0.05$), respectively, at 24 hours in stressed pups, compared with controls (Figure 5B). At 48 hours, claudin 4 expression recovered, whereas claudin 7 remained significantly down-regulated, by 45% (CI = 20% to 62%; $P < 0.05$) (Figure 5B). Claudin 2 gene expression, however, did not change at 24 and 48 hours (Figure 5B).

Claudin 2 Protein Is Elevated in Human NEC

The expression of claudin 2, claudin 4, occludin, and ZO-1 was assessed in control and human NEC tissues by immunohistochemistry. Claudin 2 expression scored low in control colon (crypt expression 1.0 ± 0.1 and surface expression 1.0 ± 0.2) and showed a decreasing gradient of expression from the crypts to the surface of small intestine (crypt expression 1.5 ± 0.3 versus surface expression 0.7 ± 0.1 ; $P < 0.05$). In human tissue samples, compared with control, claudin 2 expression was dramatically increased in the crypts of NEC colon (2 ± 0.2 versus 1.0 ± 0.1 ; $P < 0.001$) and NEC

small intestine (2.3 ± 0.2 versus 1.5 ± 0.3 ; $P < 0.05$) (Figure 6A); in these tissues, staining was strong at the TJ and also on lateral cell membranes and cytoplasm (Figure 6B). In contrast to claudin 2, expression and distribution of occludin and ZO-1 were similar in control and NEC tissues (Figure 6A). Occludin expression was strongest at the TJ, but staining could also be detected in lateral membranes and cytoplasm (Figure 6B). ZO-1 expression localized only to the region of the TJ (Figure 6B). In control tissues, claudin 4 was detected mainly on lateral membranes, but also in the cytoplasm. In NEC specimens, the cytoplasmic localization of claudin 4 was more apparent, compared with controls, although the difference did not reach statistical significance. Expression levels for claudin 4, occludin, and ZO-1 were similar between the crypts and the surface colonocytes. Crypt staining scores are presented in Figure 6A.

In Dam-Fed Controls, Claudins 2, 4, and 7 Cofractionate with Caveolin 1 in Low-Density Membranes, whereas These Proteins Predominate in High-Density Fractions in Stressed Pups

Claudin distribution was determined by Western blotting of detergent-insoluble membrane fractions. In DF controls, claudins 2, 4, and 7 cofractionated with the lipid raft protein caveolin 1. In stressed pups, the preferential localization of claudins 2 and 4 in low-density fractions was lost, and instead the proteins were found in high-density fractions (Figure 7).

Administration of *B. infantis* Preserved Claudin 4 and Occludin Distribution at TJs

In pups stressed for 12 hours (Figure 8) and 24 hours (data not shown) and in pups treated with vehicle alone (Figure 8), occludin and claudin 4 were diffusely present in the cytoplasm. In pups treated with *B. infantis* prior to the NEC protocol, claudin 4 was only weakly detected in the cytoplasm, and its concentration at TJ structures was preserved (Figure 8). Also, the association of occludin with TJs was sustained in villous enterocytes (Figure 8), and cofractionation of claudins 2 and 4 with caveolin 1 in membrane-rich fractions was preserved in these pups (Figure 9).

Administration of *B. infantis* Attenuates the Increase in Intestinal Permeability and Decreases the Incidence of NEC

The 24-hour increase in intestinal permeability (as assessed by serum FITC–dextran levels 4 hours after oral FITC–dextran administration) was significantly attenuated, by $45\% \pm 18\%$ ($P < 0.05$), in pups treated with 3×10^6 CFU *B. infantis* prior to the NEC protocol, compared with vehicle-treated controls (Figure 10). Moreover, only 9/26 pups treated with *B. infantis* developed histological evidence of severe NEC (injury

score ≥ 2), compared with 16/24 pups treated with maltodextran alone ($\chi^2 = 3.93$, $P < 0.05$) (Figure 11).

Discussion

Despite considerable advances in NEC research, the exact pathogenesis remains elusive. In other intestinal inflammatory disorders, such as Crohn's disease, an increase in intestinal permeability has been shown to precede the illness²⁴ and its relapse,²⁵ and is thought to contribute to disease pathogenesis.²⁶ In human neonates, an increase in intestinal permeability has been found in advanced stages of NEC.² In a neonatal rat NEC model, intestinal permeability is increased at 48, 72, and 96 hours.^{3,4,12,13} However, intestinal injury is commonly seen at these time points, and therefore permeability changes might be secondary to intestinal injury. In the present study, we clearly show in

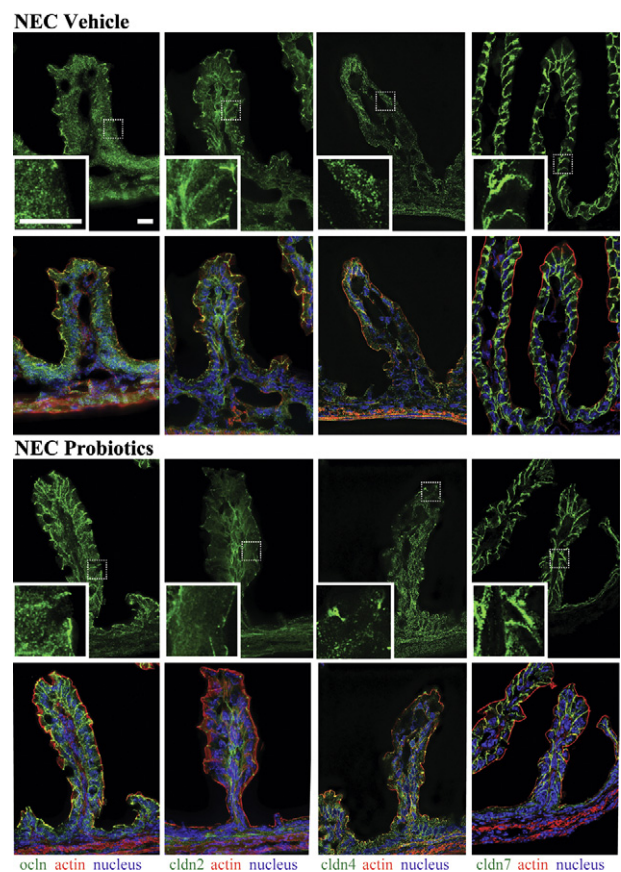


Figure 8 Administration of *B. infantis* preserved claudin 4 and occludin localization at TJs. Frozen sections of small intestines of pups treated with *B. infantis* (Probiotics group) or vehicle control (NEC group) and submitted to the NEC protocol for 12 hours were examined for claudins 2, 4, and 7 (green) and for occludin (green) by immunofluorescence (top row in each group). **Boxed regions** correspond to higher-magnification images in the **insets**. Merged images (**bottom row** in each group) also show β -actin (red) and DAPI nuclear staining (blue). In vehicle-treated pups, occludin and claudin 4 were found throughout the cytoplasm, whereas in *B. infantis*-treated mice, claudin 4 remained localized at TJs and occludin was found both in the cytoplasm and at the TJ. $n = 4$ per group. Scale bar = 40 μ m.

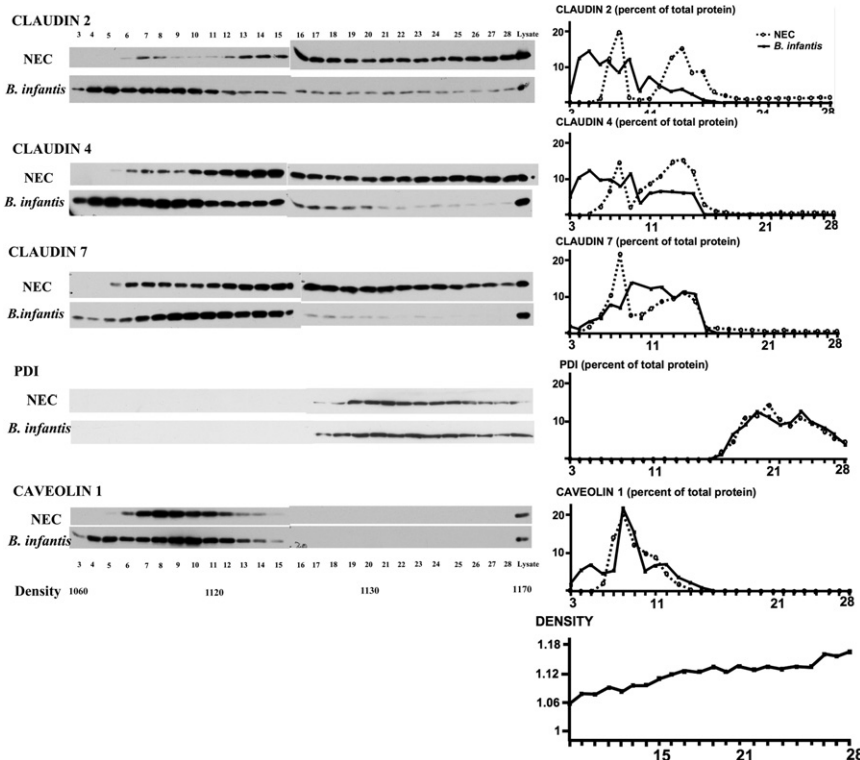


Figure 9 The localization of claudins 2, 4, and 7 to low-density fractions is preserved in *B. infantis*-treated pups, as indicated by Western blotting and quantification of claudin proteins and specific subcellular markers in small intestinal tissue fractions of stressed pups (24 hours) treated with *B. infantis* or vehicle control (NEC). Results are representative of two independent experiments, run in triplicate.

a neonatal mouse NEC model that intestinal permeability is increased before histological intestinal injury can be detected. Early increases in intestinal permeability may therefore contribute to NEC pathogenesis by allowing translocation of microbial products or their antigens to promote a mucosal inflammatory response.

Paracellular movement of water and small molecules across the epithelium is controlled by TJ complexes. These are dynamic structures, changing in response to various stimuli, including bacteria and bacterial products.²⁷ Among

the various proteins constituting TJs, members of the claudin family have been shown to regulate paracellular permeability.⁸ Claudin 2 increases the permeability of small ions and molecules,²⁸ and removal of claudin 4 is associated with an increase in epithelial permeability and disruption of fibril organization in Madin–Darby canine kidney cells.²⁹ During development, TJ complexes have been detected in the human intestine as early as 10 weeks of gestation³⁰ and, in the neonatal mouse intestine, claudin gene expression is developmentally regulated.³¹ Murine paracellular permeability is elevated in 1-week-old mouse pups and decreases significantly during postnatal maturation.³² TJ proteins are redistributed during several disease processes.^{11,33} In colonic biopsies from patients with ulcerative colitis, loss of claudin 4 association with TJs has been reported,¹¹ and claudin 2 is increased in inflammatory bowel disease.²¹ In studies using a neonatal rat model of NEC, the expression of claudin 3 was increased at 72 and 96 hours in the intestine of stressed pups, compared with controls.^{3,12,13} The association of ZO-1 with TJ was lost in a neonatal rat model at day 5.¹²

Whether changes in the expression and distribution of specific TJ proteins precede the intestinal injury in NEC remains unclear. In the present study, the integrity of TJ structures was maintained in enterocytes in pups stressed for 24 hours, but the apical-to-basolateral TJ length was greater than in DF controls, consistent with TJ restructuring. In pups stressed for 12 hours, the association of claudin 4 with TJs was markedly decreased, and occludin and claudin 4 were detected throughout the cytoplasm. At 24 and 72 hours,

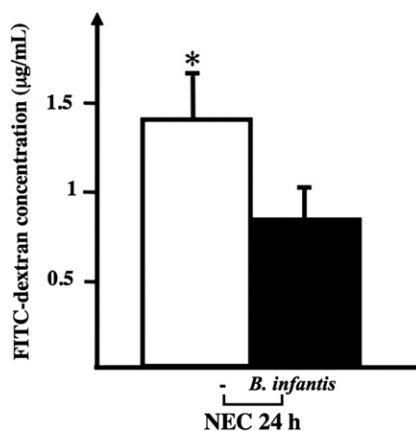


Figure 10 Administration of *B. infantis* attenuated the increase in intestinal permeability in pups stressed for 24 hours. Serum FITC-dextran concentration 4 hours after orogastric administration was lower in mice submitted to the NEC protocol for 24 hours and treated with *B. infantis*, compared with vehicle control (–). Data are expressed as means \pm SEM. $n = 11$ to 13 per group. * $P < 0.05$.

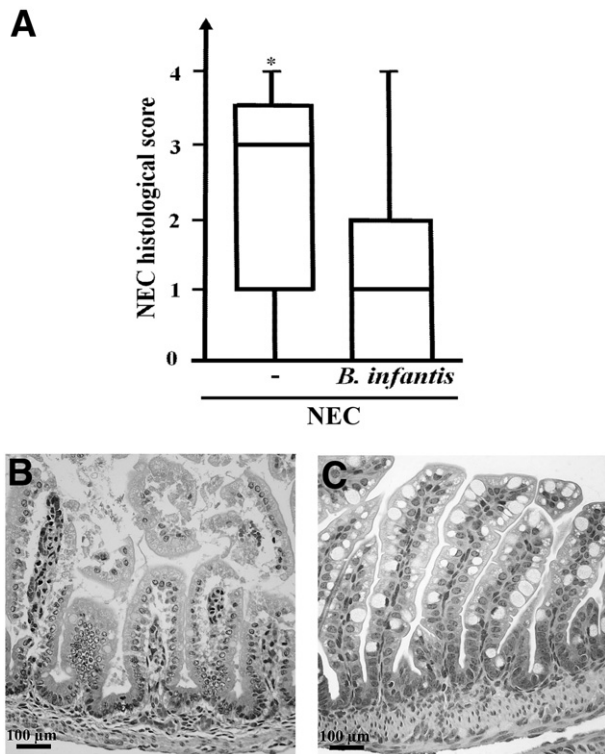


Figure 11 Administration of *B. infantis* significantly decreased the incidence of NEC in a mouse model. **A:** NEC histological scores of mice submitted to the NEC protocol for 72 hours and treated with *B. infantis* or vehicle alone (—). **B** and **C:** Typical appearance of the small intestine of an untreated pup (**B**) showing evidence of grade 2 NEC, compared with the small intestine of a pup treated with *B. infantis* (**C**) and showing intact villi. Data are expressed as box-and-whisker plots, indicating median, interquartile range, and minimum and maximum values. $n = 26$ or 27 per group. $*P < 0.05$.

claudin 2 and claudin 7 were also found in the cytoplasm. In contrast, in DF controls, claudin 2, claudin 4, and occludin were densely localized to TJ structures, and claudin 7 was associated mainly with enterocyte lateral membranes.

Whether redistribution of claudins 2, 4, and 7 in experimental NEC is accompanied by changes in total amount of TJ proteins remains unknown. In the present study, we found an increase in claudin 2, but no change in levels of claudins 4 and 7 in stressed pups, compared with DF controls. We also found that claudin 2 was elevated in human NEC surgical samples. This is similar to what has been reported in human inflammatory bowel disease, where claudin 2 is highly present in inflamed colonic tissue but is barely detectable in normal colon.^{11,21} Claudin 2 increases paracellular channel-like permeability to monovalent cations,³⁴ and IL-6 increases TJ permeability by stimulating the expression of pore-forming claudin 2.³⁵ It is unclear whether the increase in claudin 2 is injurious, or perhaps serves as a compensatory protective mechanism. For example, increased Na permeability and subsequent absorption of nutrients such as glucose and amino acids may be beneficial, by limiting malnutrition during a time of stress. Furthermore, increased paracellular Na flux may promote passive paracellular loss of water, thus serving as a flushing mechanism for pathogens.

It remains unknown whether the maintenance of steady-state levels of claudins 4 and 7 and increase in claudin 2 found in our NEC model is due to increased transcription. In the present study, claudin 2 mRNA was up-regulated at 6 hours, but claudin 4 and 7 mRNA was not. Indeed, in stressed pups, claudin 4 and 7 expression was significantly down-regulated at 24 hours, compared with DF controls, and expression of claudin 2 was unchanged. Our results are similar to what has been reported in biopsies of patients with active ulcerative colitis.³⁶ This led us to hypothesize that claudins 4 and 7 are recycled in the enterocytes of stressed animals.

We confirmed internalization of claudins 2, 4, and 7 in experimental NEC using subcellular density gradient fractionation. In DF controls, claudins 2, 4, and 7 cofractionated with the lipid raft marker caveolin 1 in low-density fractions. In stressed pups, however, these claudins lost their association with membrane-rich fractions and were found mainly in high-density fractions. Similarly, it has been reported that sepsis causes claudins to be displaced from raft fractions to nonraft fractions, suggesting internalization of these proteins.³³ In a neonatal rat NEC model, claudin 3 relocated from the membrane of the enterocytes to the cytosol.³⁷

There is strong evidence from both human trials¹⁸ and animal studies¹⁷ that the administration of probiotics, such as *Lactobacillus acidophilus* and *B. infantis*, protects against NEC when administered prophylactically to preterm newborns. However, the mechanisms remain poorly understood. In a model of colitis induced by dextran sodium sulfate, treatment with *B. infantis* protected the epithelial barrier and decreased the inflammatory response.^{38,39} In T84 human colonic adenocarcinoma cells, treatment with *B. infantis*-conditioned medium resulted in increased expression of claudin 4, ZO-1, and occludin, as well as decreased levels of claudin 2.³⁹ *B. infantis* also prevented IFN- γ -induced rearrangement of occludin and claudin 1 in T84 monolayers.³⁹ In a neonatal rat NEC model, *B. bifidum* partially reduced stress-induced relocation of claudin-3 to the cytoplasm and preserved its association with the membrane of enterocytes in the crypt.³⁷ In 2-week-old mice, enteral administration of *L. rhamnosus* strain GG accelerated intestinal barrier maturation and induced expression of claudin 3.³²

In the present study, using neonatal mice, we clearly show that *B. infantis* not only preserved claudin 4 and occludin integrity at TJ structures, but also markedly attenuated the increase in intestinal permeability observed at 24 hours and decreased the incidence of severe NEC. These findings concur with a human study conducted with preterm infants, in which bifidobacterial supplementation of formula with *B. animalis lactis* (previously *B. lactis*) decreased intestinal permeability at day of life 30.⁴⁰

In conclusion, we have demonstrated that increased intestinal permeability precedes NEC in a neonatal mouse model. This permeability change is associated with increased expression of claudin 2 and internalization of claudin 4 and occludin. Claudin 2 was elevated also in human NEC. In the mouse NEC model, although the ultrastructural integrity of

enterocyte TJ structures was maintained, the TJ length in NEC tissues was greater, consistent with restructuring of the TJ. Administration of *B. infantis* prevented the increase in intestinal permeability and preserved claudin 4 and occludin localization at TJ structures. These effects were associated with a decreased incidence of NEC in our neonatal mouse model. Thus, the protective effect of *B. infantis* on NEC may be due, at least in part, to enhanced intestinal barrier function and preservation of TJ molecular structures. These data suggest that interventions aimed at preserving the intestinal barrier, including probiotic therapy, may be useful in preventing NEC.

Acknowledgment

We thank Dr. Amanda Marchiando for technical support.

References

- Lin PW, Stoll BJ: Necrotizing enterocolitis. *Lancet* 2006, 368:1271–1283
- Piena-Spoel M, Albers MJ, ten Kate J, Tibboel D: Intestinal permeability in newborns with necrotizing enterocolitis and controls: does the sugar absorption test provide guidelines for the time to (re-)introduce enteral nutrition? *J Pediatr Surg* 2001, 36:587–592
- Clark JA, Doelle SM, Halpern MD, Saunders TA, Holubec H, Dvorak K, Boitano SA, Dvorak B: Intestinal barrier failure during experimental necrotizing enterocolitis: protective effect of EGF treatment. *Am J Physiol Gastrointest Liver Physiol* 2006, 291:G938–G949
- Feng J, El Assal ON, Besner GE: Heparin-binding epidermal growth factor-like growth factor decreases the incidence of necrotizing enterocolitis in neonatal rats. *J Pediatr Surg* 2006, 41:144–149
- Arrieta MC, Bistritz L, Meddings JB: Alterations in intestinal permeability. *Gut* 2006, 55:1512–1520
- Colegio OR, Van Itallie C, Rahner C, Anderson JM: Claudin extracellular domains determine paracellular charge selectivity and resistance but not tight junction fibril architecture. *Am J Physiol Cell Physiol* 2003, 284:C1346–C1354
- Van Itallie C, Rahner C, Anderson JM: Regulated expression of claudin-4 decreases paracellular conductance through a selective decrease in sodium permeability. *J Clin Invest* 2001, 107:1319–1327
- Furuse M, Hata M, Furuse K, Yoshida Y, Haratake A, Sugitani Y, Noda T, Kubo A, Tsukita S: Claudin-based tight junctions are crucial for the mammalian epidermal barrier: a lesson from claudin-1-deficient mice. *J Cell Biol* 2002, 156:1099–1111
- Viswanathan VK, Weffen A, Koutsouris A, Roxas JL, Hecht G: Enteropathogenic *E. coli*-induced barrier function alteration is not a consequence of host cell apoptosis. *Am J Physiol Gastrointest Liver Physiol* 2008, 294:G1165–G1170
- Ivanov AI, Nusrat A, Parkos CA: The epithelium in inflammatory bowel disease: potential role of endocytosis of junctional proteins in barrier disruption. *Novartis Found Symp* 2004, 263:115–124
- Prasad S, Mingrino R, Kaukinen K, Hayes KL, Powell RM, MacDonald TT, Collins JE: Inflammatory processes have differential effects on claudins 2, 3 and 4 in colonic epithelial cells. *Lab Invest* 2005, 85:1139–1162
- Shiou SR, Yu Y, Chen S, Ciancio MJ, Petrof EO, Sun J, Claud EC: Erythropoietin protects intestinal epithelial barrier function and lowers the incidence of experimental neonatal necrotizing enterocolitis. *J Biol Chem* 2011, 286:12123–12132
- Rentea RM, Liedel JL, Welak SR, Cassidy LD, Mayer AN, Pritchard KA Jr, Oldham KT, Gourlay DM: Intestinal alkaline phosphatase administration in newborns is protective of gut barrier function in a neonatal necrotizing enterocolitis rat model. *J Pediatr Surg* 2012, 47:1135–1142
- Tannock GW: The normal microflora: an introduction. *Medical Importance of the Normal Microflora*. Edited by Tannock GW. Dordrecht, The Netherlands, Kluwer Academic Publishers, 1999, pp 1–23
- Fanaro S, Chierici R, Guerrini P, Vigi V: Intestinal microflora in early infancy: composition and development. *Acta Paediatr Suppl* 2003, 91:48–55
- Butel MJ, Suau A, Campeotto F, Magne F, Aires J, Ferraris L, Kalach N, Leroux B, Dupont C: Conditions of bifidobacterial colonization in preterm infants: a prospective analysis. *J Pediatr Gastroenterol Nutr* 2007, 44:577–582
- Caplan MS, Miller-Catchpole R, Kaup S, Russell T, Lickerman M, Am M, Xiao Y, Thomson R Jr: Bifidobacterial supplementation reduces the incidence of necrotizing enterocolitis in a neonatal rat model. *Gastroenterology* 1999, 117:577–583
- Lin HC, Su BH, Chen AC, Lin TW, Tsai CH, Yeh TF, Oh W: Oral probiotics reduce the incidence and severity of necrotizing enterocolitis in very low birth weight infants. *Pediatrics* 2005, 115:1–4
- Boirivant M, Strober W: The mechanism of action of probiotics. *Curr Opin Gastroenterol* 2007, 23:679–692
- Tian R, Liu SXL, Williams C, Soltau TD, Dimmitt R, Zheng X, De Plaen IG: Characterization of a necrotizing enterocolitis model in newborn mice. *Int J Clin Exp Med* 2010, 3:293–302
- Weber CR, Nalle SC, Tretiakova M, Rubin DT, Turner JR: Claudin-1 and claudin-2 expression is elevated in inflammatory bowel disease and may contribute to early neoplastic transformation. *Lab Invest* 2008, 88:1110–1120
- Liu SXL, Tian R, Baskind H, Hsueh W, De Plaen IG: Platelet-activating factor induces the processing of nuclear factor-kappaB p105 into p50, which mediates acute bowel injury in mice. *Am J Physiol Gastrointest Liver Physiol* 2009, 297:G76–G81
- Clayburgh DR, Barrett TA, Tang Y, Meddings JB, Van Eldik LJ, Watterson DM, Clarke LL, Mrsny RJ, Turner JR: Epithelial myosin light chain kinase-dependent barrier dysfunction mediates T cell activation-induced diarrhea in vivo. *J Clin Invest* 2005, 115:2702–2715
- Irvine EJ, Marshall JK: Increased intestinal permeability precedes the onset of Crohn's disease in a subject with familial risk. *Gastroenterology* 2000, 119:1740–1744
- Arnott ID, Kingstone K, Ghosh S: Abnormal intestinal permeability predicts relapse in inactive Crohn disease. *Scand J Gastroenterol* 2000, 35:1163–1169
- McGuckin MA, Eri R, Simms LA, Florin TH, Radford-Smith G: Intestinal barrier dysfunction in inflammatory bowel diseases. *Inflamm Bowel Dis* 2009, 15:100–113
- Nusrat A, Turner JR, Madara JL: Molecular physiology and pathophysiology of tight junctions. IV. Regulation of tight junctions by extracellular stimuli: nutrients, cytokines, and immune cells. *Am J Physiol Gastrointest Liver Physiol* 2000, 279:G851–G857
- Muto S, Hata M, Taniguchi J, Tsuruoka S, Moriwaki K, Saitou M, Furuse K, Sasaki H, Fujimura A, Imai M, Kusano E, Tsukita S, Furuse M: Claudin-2-deficient mice are defective in the leaky and cation-selective paracellular permeability properties of renal proximal tubules. *Proc Natl Acad Sci USA* 2010, 107:8011–8016
- Sonoda N, Furuse M, Sasaki H, Yonemura S, Katahira J, Horiguchi Y, Tsukita S: Clostridium perfringens enterotoxin fragment removes specific claudins from tight junction strands: evidence for direct involvement of claudins in tight junction barrier. *J Cell Biol* 1999, 147:195–204
- Polak-Charcon S, Shoham J, Ben-Shaul Y: Tight junctions in epithelial cells of human fetal hindgut, normal colon, and colon adenocarcinoma. *J Natl Cancer Inst* 1980, 65:53–62
- Holmes JL, Van Itallie CM, Rasmussen JE, Anderson JM: Claudin profiling in the mouse during postnatal intestinal development and along the gastrointestinal tract reveals complex expression patterns. *Gene Expr Patterns* 2006, 6:581–588

32. Patel RM, Myers LS, Kurundkar AR, Maheshwari A, Nusrat A, Lin PW: Probiotic bacteria induce maturation of intestinal claudin 3 expression and barrier function [Erratum appeared in *Am J Pathol* 2012, 180:1324]. *Am J Pathol* 2012, 180:626–635
33. Li Q, Zhang Q, Wang C, Liu X, Li N, Li J: Disruption of tight junctions during polymicrobial sepsis in vivo. *J Pathol* 2009, 218:210–221
34. Tamura A, Hayashi H, Imasato M, Yamazaki Y, Hagiwara A, Wada M, Noda T, Watanabe M, Suzuki Y, Tsukita S: Loss of claudin-15, but not claudin-2, causes Na⁺ deficiency and glucose malabsorption in mouse small intestine. *Gastroenterology* 2011, 140:913–923
35. Suzuki T, Yoshinaga N, Tanabe S: Interleukin-6 (IL-6) regulates claudin-2 expression and tight junction permeability in intestinal epithelium. *J Biol Chem* 2011, 286:31263–31271
36. Oshima T, Miwa H, Joh T: Changes in the expression of claudins in active ulcerative colitis. *J Gastroenterol Hepatol* 2008, 23(Suppl 2): S146–S150
37. Khailova L, Dvorak K, Arganbright KM, Halpern MD, Kinouchi T, Yajima M, Dvorak B: Bifidobacterium bifidum improves intestinal integrity in a rat model of necrotizing enterocolitis. *Am J Physiol Gastrointest Liver Physiol* 2009, 297:G940–G949
38. Fitzpatrick LR, Hertzog KL, Quatse AL, Koltun WA, Small JS, Vrana K: Effects of the probiotic formulation VSL#3 on colitis in weanling rats. *J Pediatr Gastroenterol Nutr* 2007, 44:561–570
39. Ewaschuk JB, Diaz H, Meddings L, Diederichs B, Dmytrash A, Backer J, Looijer-van LM, Madsen KL: Secreted bioactive factors from Bifidobacterium infantis enhance epithelial cell barrier function. *Am J Physiol Gastrointest Liver Physiol* 2008, 295: G1025–G1034
40. Stratiki Z, Costalos C, Sevastiadou S, Kastanidou O, Skouroliahou M, Giakoumatou A, Petrohilou V: The effect of a bifidobacter supplemented bovine milk on intestinal permeability of preterm infants. *Early Hum Dev* 2007, 83:575–579